

Review and Demonstration of a Mixture Representation for Simulation from Densities Involving Sums of Powers

Maryclare Griffin

August 6, 2024

Abstract

Penalized and robust regression, especially when approached from a Bayesian perspective, can involve the problem of simulating a random variable \mathbf{z} from a posterior distribution that includes a term proportional to a sum of powers, $\|\mathbf{z}\|_q^q$, on the log scale. However, many popular gradient-based methods for Markov Chain Monte Carlo simulation from such posterior distributions use Hamiltonian Monte Carlo and accordingly require conditions on the differentiability of the unnormalized posterior distribution that do not hold when $q \leq 1$ (Plummer, 2023). This is limiting; the setting where $q \leq 1$ includes widely used sparsity inducing penalized regression models and heavy tailed robust regression models. In the special case where $q = 1$, a latent variable representation that facilitates simulation from such a posterior distribution is well known. However, the setting where $q < 1$ has not been treated as thoroughly. In this note, we review the availability of a latent variable representation described in Devroye (2009), show how it can be used to simulate from such posterior distributions when $0 < q < 2$, and demonstrate its utility in the context of estimating the parameters of a Bayesian penalized regression model.

Keywords: Exponential power distribution, bridge estimator, stable distribution, scale mixture, generalized normal distribution, robust regression.

¹Department of Mathematics and Statistics, University of Massachusetts Amherst, Amherst, MA 01003 (maryclaregri@umass.edu).

This research was supported by NSF grant DMS-2113079. Associated code is available at <https://github.com/maryclare/EPStan>. The author gratefully acknowledges helpful comments from Hanyu Xiao.

1 Introduction

Consider the problem of simulating a length- n random variable \mathbf{z} from a distribution with density $p(\mathbf{z}) \propto \exp\{-f(\mathbf{z})\}$. Modern methods, specifically gradient-based methods such as Hamiltonian Monte Carlo (HMC), may either require or greatly benefit from the following: (i) differentiability of $f(\mathbf{z})$ and (ii) availability of a closed form expression for $f(\mathbf{z})$ (Plummer, 2023; Štrumbelj et al., 2024). Letting $g(\mathbf{z})$ refer to the part of $f(\mathbf{z})$ that is differentiable and partitioning $\mathbf{z} = (\mathbf{z}_1, \mathbf{z}_2)$ into two components \mathbf{z}_1 and \mathbf{z}_2 of length n_1 and n_2 , a common form of $f(\mathbf{z})$ that violates (i) is given by

$$f(\mathbf{z}) = g(\mathbf{z}) + \lambda \|\mathbf{z}_2\|_q^q \tag{1}$$

when $q \leq 1$. This arises in many settings including robust and penalized regression (Poirier et al., 1986; Butler et al., 1990; Frank and Friedman, 1993; Polson et al., 2014).

A well known way of addressing this problem in the case of $q = 1$ is to leverage the scale mixture representation of the density proportional to $\exp\{-\lambda\|\mathbf{z}_2\|_1\}$ (West, 1987; Park and Casella, 2008; Hans, 2009; Ding and Blitzstein, 2018). Specifically, when \mathbf{z}_2 has a density proportional to $\exp\{-\lambda\|\mathbf{z}_2\|_1\}$, we can equivalently write that $z_{2i}|v_i \sim \text{normal}(0, v_i/\lambda)$ where $v_i \sim \text{exponential}(1/2)$. Accordingly, we can simulate \mathbf{z} according to the density proportional to $\exp\{-g(\mathbf{z}) - \lambda\|\mathbf{z}_2\|_1\}$ by simulating \mathbf{z} and \mathbf{v} according to the density proportional to

$$\exp\left\{-g(\mathbf{z}) - \frac{1}{2}(\mathbf{1}'\log(\mathbf{v})) - \frac{\lambda}{2}(\mathbf{z}'_2 \text{diag}\{\mathbf{v}\}^{-1} \mathbf{z}_2) - \frac{1}{2}(\mathbf{1}'\mathbf{v})\right\}.$$

This is helpful because $(\mathbf{1}'\log(\mathbf{v}))/2 + \lambda(\mathbf{z}'_2 \text{diag}\{\mathbf{v}\}^{-1} \mathbf{z}_2)/2 + (\mathbf{1}'\mathbf{v})/2$ is a differentiable function of \mathbf{z}_2 and \mathbf{v} . This representation has been used extensively for Bayesian computation (Park and Casella, 2008; Hans, 2009).

When $q \neq 1$ and when \mathbf{z}_2 has a density proportional to $\exp\{-\lambda\|\mathbf{z}_2\|_q^q\}$, the equivalent normal scale mixture representation is $z_{2i}|v_i \sim \text{normal}(0, v_i/\lambda^{2/q})$ where v_i are independent and polynomially tilted positive α -stable distribution with index of stability $\alpha = q/2$ (West, 1987). An analogous approach simulates \mathbf{z} according to the density proportional to

$\exp\{-g(\mathbf{z}) - \lambda\|\mathbf{z}_2\|_q^q\}$ by simulating \mathbf{z} and \mathbf{v} according to the density proportional to

$$\exp\left\{-g(\mathbf{z}) - \frac{1}{2}(\mathbf{1}'\log(\mathbf{v})) - \frac{\lambda^{\frac{2}{q}}}{2}(\mathbf{z}'_2\text{diag}\{\mathbf{v}\}^{-1}\mathbf{z}_2) - \mathbf{1}'h(\mathbf{v};q)\right\},$$

where $h(\mathbf{v};q)$ is a function that does not have a closed form expression (Polson et al., 2014).

This can be resolved by further recognizing the distribution of the scales v_i as a rate mixtures of generalized gamma random variables (Devroye, 2009). We can write polynomially titled positive α -stable v_i as equal in distribution to a transformation of gamma and Zolotarev distributed random variables $\xi_i > 0$ and $0 < \delta_i < \pi$,

$$v_i \stackrel{d}{=} \frac{1}{2} \left(\xi_i^{\frac{2-q}{q}} \sin\left(\left(\frac{q}{2}\right)\delta_i\right)^{-1} \sin\left(\left(\frac{2-q}{2}\right)\delta_i\right)^{\frac{q-2}{q}} \sin(\delta_i)^{\frac{2}{q}} \right),$$

$\xi_i \stackrel{i.i.d.}{\sim}$ gamma $\left(\text{shape} = \frac{2+q}{2q}, \text{rate} = 1\right)$ and

$$p(\delta_i|q) = \left(\frac{\Gamma(1 + \frac{1}{2}) \Gamma(\frac{1}{2} + \frac{1}{q})}{\pi \Gamma(1 + \frac{1}{q})} \right) \sin\left(\left(\frac{q}{2}\right)\delta_i\right)^{-\frac{1}{2}} \sin\left(\left(\frac{2-q}{2}\right)\delta_i\right)^{\frac{q-2}{2q}} \sin(\delta_i)^{\frac{1}{q}}.$$

This implies that we can simulate \mathbf{z} according to the density proportional to $\exp\{-g(\mathbf{z}) - \lambda\|\mathbf{z}_2\|_q^q\}$ by simulating \mathbf{z} , $\boldsymbol{\xi}$, and $\boldsymbol{\delta}$ according to the density proportional to

$$\exp\left\{-g(\mathbf{z}) - \lambda^{\frac{2}{q}} \left(\mathbf{1}' \left(\boldsymbol{\xi}^{\frac{q-2}{q}} \circ \sin\left(\left(\frac{q}{2}\right)\boldsymbol{\delta}\right) \circ \sin\left(\left(\frac{2-q}{2}\right)\boldsymbol{\delta}\right)^{\frac{2-q}{q}} \circ \sin(\boldsymbol{\delta})^{-\frac{2}{q}} \circ \mathbf{z}_2^2 \right) \right) - \mathbf{1}'\boldsymbol{\xi} \right\}, \quad (2)$$

where ‘ \circ ’ refers to the elementwise Hadamard product and $\sin(\cdot)$ and $(\cdot)^a$ are applied elementwise. This is differentiable with respect to \mathbf{z} , $\boldsymbol{\xi}$, and $\boldsymbol{\delta}$. A derivation which includes the normalizing constant $C(q, \lambda) = \int \exp\{-\lambda\|\mathbf{z}_q\|_q^q\} d\mathbf{z}_2$ is provided in an Appendix.

In some situations, alternative “non-centered” parametrization may be preferable (Bentancourt and Girolami, 2015). We can simulate \mathbf{z} according to the density proportional to $\exp\{-g(\mathbf{z}) - \lambda\|\mathbf{z}_2\|_q^q\}$ by simulating \mathbf{z}_1 , \mathbf{w} , $\boldsymbol{\xi}$, and $\boldsymbol{\delta}$ according to the density proportional

to

$$\begin{aligned} \exp \left\{ -g \left(\left(\mathbf{z}_1, 2^{-\frac{1}{2}} \lambda^{-\frac{1}{q}} \left(\boldsymbol{\xi}^{\frac{2-q}{2q}} \circ \sin \left(\left(\frac{q}{2} \right) \boldsymbol{\delta} \right)^{-\frac{1}{2}} \circ \sin \left(\left(\frac{2-q}{2} \right) \boldsymbol{\delta} \right)^{\frac{q-2}{2q}} \circ \sin(\boldsymbol{\delta})^{\frac{1}{q}} \circ \mathbf{w} \right) \right) \right) \right\} + \quad (3) \\ - \left(\frac{1}{2} \right) \mathbf{w}' \mathbf{w} + \left(\frac{2-q}{2q} \right) \mathbf{1}' \log(\boldsymbol{\xi}) - \mathbf{1}' \boldsymbol{\xi} + \left(\frac{q-2}{2q} \right) \mathbf{1}' \log \left(\sin \left(\left(\frac{2-q}{2} \right) \boldsymbol{\delta} \right) \right) + \\ - \left(\frac{1}{2} \right) \mathbf{1}' \log \left(\sin \left(\left(\frac{q}{2} \right) \boldsymbol{\delta} \right) \right) + \left(\frac{1}{q} \right) \mathbf{1}' \log(\sin(\boldsymbol{\delta})) \left. \right\}, \end{aligned}$$

and setting $\mathbf{z}_2 = 2^{-1/2} \lambda^{-1/q} (\boldsymbol{\xi}^{\frac{2-q}{2q}} \circ \sin(q\boldsymbol{\delta}/2)^{-1/2} \circ \sin((2-q)\boldsymbol{\delta}/2)^{(q-2)/(2q)} \circ \sin(\boldsymbol{\delta})^{1/q} \circ \mathbf{w})$.

Analogously, this is differentiable with respect to \mathbf{z}_1 , \mathbf{w} , $\boldsymbol{\xi}$, and $\boldsymbol{\delta}$. As before, derivation which includes the normalizing constant is provided in an Appendix.

2 Demonstration

We demonstrate the use of these representations for simulation of regression coefficients \mathbf{z}_2 under a penalized regression model relating an $m \times 1$ response \mathbf{y} to an $m \times n_2$ matrix of covariates \mathbf{X} via unknown parameters $\boldsymbol{\theta} = (\sigma^2, \lambda, q)$,

$$\mathbf{y} = \mathbf{X} \mathbf{z}_2 + \mathbf{e}, \quad p(\mathbf{z}_2) \propto \exp \left\{ -\lambda \|\mathbf{z}_2\|_q^q \right\}, \quad \mathbf{e} \sim \text{normal}(\mathbf{0}, \sigma^2 \mathbf{I}_m), \quad (4)$$

where \mathbf{I}_m refers to an $m \times m$ identity matrix. When $\boldsymbol{\theta}$ is fixed, the penalized regression model (4) has $g(\mathbf{z}) = -\|\mathbf{y} - \mathbf{X} \mathbf{z}_2\|_2^2 / (2\sigma^2)$ and $\mathbf{z} = \mathbf{z}_2$.

We consider two datasets that are frequently used in the relevant literature, which we refer to as the prostate and glucose data, respectively. Because the performance of algorithms for simulating from simulating a random variable is known to depend on the dimension of the random variable, the two datasets are chosen to exemplify simulation of a relatively low dimensional random variable, with dimension $n_2 = 8$, and a relatively high dimensional random variable, with dimension $n_2 = 72$. The prostate data has appeared in Tibshirani (1996) and contains measurements of log prostate specific antigen and $n_2 = 8$ clinical measures associated with prostate cancer progression for $m = 97$ subjects. The glucose data has appeared in Priami and Morine (2015) and contains measurements of blood glucose concentration and

$n_2 = 72$ metabolite measurements and health indicators for $m = 68$ subjects.

We consider 9 values of $\boldsymbol{\theta} = (\sigma^2, \lambda, q)$ to compare the performance of methods for simulating from the posterior distribution of \mathbf{z}_2 , denoted by $\boldsymbol{\theta}^{(1)}, \dots, \boldsymbol{\theta}^{(9)}$. We estimate some components of each $\boldsymbol{\theta}^{(k)}$ from the data and systematically vary others. We obtain estimates $\hat{\sigma}^2$ and $\hat{\tau}^2$ of the noise variance and the variance of the regression coefficients \mathbf{z}_2 by minimizing

$$\log \left(|\mathbf{X} \mathbf{X}' \tau^2 + \mathbf{I} \sigma^2| \right) / 2 + \mathbf{y}' (\mathbf{X} \mathbf{X}' \tau^2 + \mathbf{I} \sigma^2)^{-1} \mathbf{y}$$

with respect to σ^2 and τ^2 . We set $\theta_1^{(k)} = \hat{\sigma}^2$, $\theta_2^{(k)} = (\Gamma(3/\theta_3^{(k)})/(\hat{\tau}^2 \Gamma(1/\theta_3^{(k)})))^{\theta^{(k)}/2}$, and $\theta_3^{(k)} = 2k/10$, which fixes the prior variance of \mathbf{z}_2 to $\hat{\tau}^2$ as in (Griffin and Hoff, 2020).

For each $\boldsymbol{\theta}^{(k)}$, we simulate from the posterior distribution of \mathbf{z}_2 under the model described by Equation (4) using STAN without changing the default settings (Carpenter et al., 2017). We compare posterior simulation using Representation (2) which we refer to as the *centered* parametrization, posterior simulation using Representation 3 which we refer to as the *non-centered* parametrization, and posterior simulation directly from (1) which we refer to as the *naive* parametrization. For each, we obtain 10 chains. Each chain simulates 1,000 burn-in (warmup) iterations followed by 1,000 draws which are retained. Starting values for \mathbf{z}_2 are shared across methods, i.e. the first chain for all three posterior simulation methods for the same data and parameters $\boldsymbol{\theta}^{(k)}$ shares the same starting value for \mathbf{z}_2 .

First, we compare estimates of the posterior mean of the log unnormalized posterior $\hat{E}[\|\mathbf{y} - \mathbf{X} \mathbf{z}_2\|_2^2 / (2\sigma^2) + \lambda \|\mathbf{z}_2\|_q^q | \mathbf{y}]$ based on the 1,000 simulated values retained after burn-in for each chain. These are shown in the first column of Figure 1. Parametrizations that correspond to better simulation from the posterior are expected to produce estimates that are less variable across chains. All three parametrizations produce estimates that are very consistent across chains when $q \geq 0.8$. When $q < 0.8$ and n_2 is relatively small, the naive and centered parametrizations (1) and (2) produce more variable estimates of the log unnormalized posterior across chains, moreso for smaller values of q . When $q < 0.8$ and n_2 is relatively large, the naive and centered parametrizations (1) and (2) not only produce

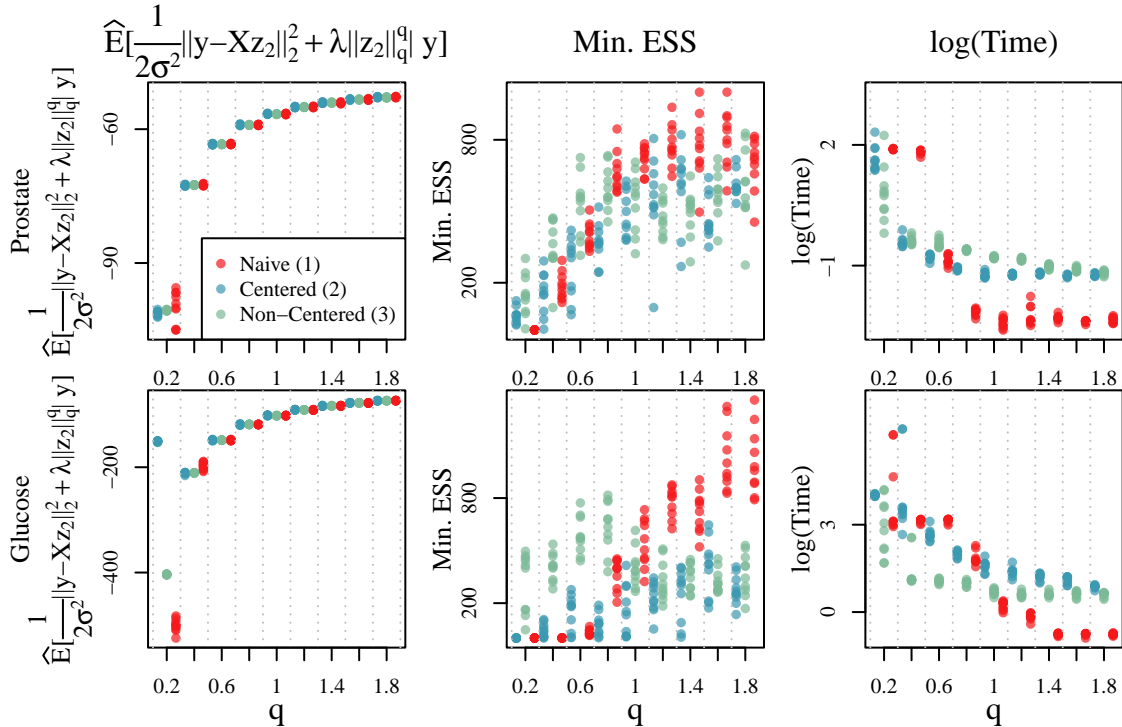


Figure 1: Estimated posterior mean log unnormalized posterior $\hat{E}[\frac{1}{2\sigma^2}\|y - Xz_2\|_2^2 + \lambda\|z_2\|_q^q | y]$, minimum effective sample size over all simulated parameters across 1,000 draws per chain after burn-in, and total time elapsed per chain for the centered parametrization (2), the non-centered parametrization 3, and the naive parametrization (1) computed from the prostate and glucose datasets.

more variable estimates of the log unnormalized posterior across chains for some values of q but also produce very different estimates of the log unnormalized posterior for others when different parametrizations are used.

The second column shows minimum effective sample sizes based on the 1,000 simulated values retained after burn-in for each chain. It suggests that the naive and centered parametrizations (1) and (2) tend to provide smaller effective sample sizes and poorer simulation from the posterior when $q \leq 0.8$. The performance of the naive and centered parametrizations (1) and (2) deteriorates as q decreases, regardless of the dimension. In particular, the minimum effective sample sizes are nearly zero when the naive or centered parametrization (1) or (2) are used. This indicates that the discordant estimates of the log unnormalized posterior across parametrizations observed for $q = 0.2$ and $n_2 = 64$ reflect

that the estimates produced by the naive and centered parametrizations (1) and (2) are incorrect, despite being precise. Unsurprisingly, we observe that the naive parametrization (1) tends to outperform the others when $q > 1$, moreso as q increases and moreso when the dimension n_2 is greater. Interestingly, when $n_2 = 8$, the naive parametrization (1) performs competitively for $q = 0.8$ and tends to perform best when $q = 1$. This is not the case when the dimension n_2 is larger, and suggesting that simulating from a log posterior that is not differentiable using the naive parametrization (1) may be more feasible when the dimension is smaller and/or when the differentiable part $g(\mathbf{z})$ of the unnormalized log posterior $f(\mathbf{z})$ dominates more.

Last, the third column of Figure 1 shows that larger effective sample sizes are not costly to obtain in terms of computation time; the parametrizations that produce the largest minimum effective sample sizes tend to have the fastest run times. The results shown in Figure 1 for $q > 1$ also highlight the cost of introducing $2 \times n_2$ additional auxiliary random variables. This adds both time and reduces efficiency, as posterior simulation with auxiliary random variables tends to take longer and produce lower effective sample sizes given the same number of simulated values.

Figure 2 helps us better understand what is happening when $q = 0.2$ for both datasets by showing kernel density estimates of the unnormalized log posterior $\|\mathbf{y} - \mathbf{X}\mathbf{z}_2\|_2^2/(2\sigma^2) + \lambda\|\mathbf{z}_2\|_q^q$ computed using the 1,000 simulated values of \mathbf{z}_2 retained after burn-in for each chain. Based on the high effective sample sizes and consistency across chains of the non-centered parametrization (3) observed in Figure 1, we treat the kernel density estimates obtained by using the non-centered parametrization (3) as a benchmark or gold standard for both datasets. This is further supported by the similarity of kernel density estimates obtained from using the non-centered parametrization (3) across chains. When the dimension n_2 is relatively small, we see that all kernel density estimates share similar supports. However, the chains obtained using the naive parametrization (1) are very heterogenous, with distinct modes and shapes which are not consistent with the kernel density estimates obtained from

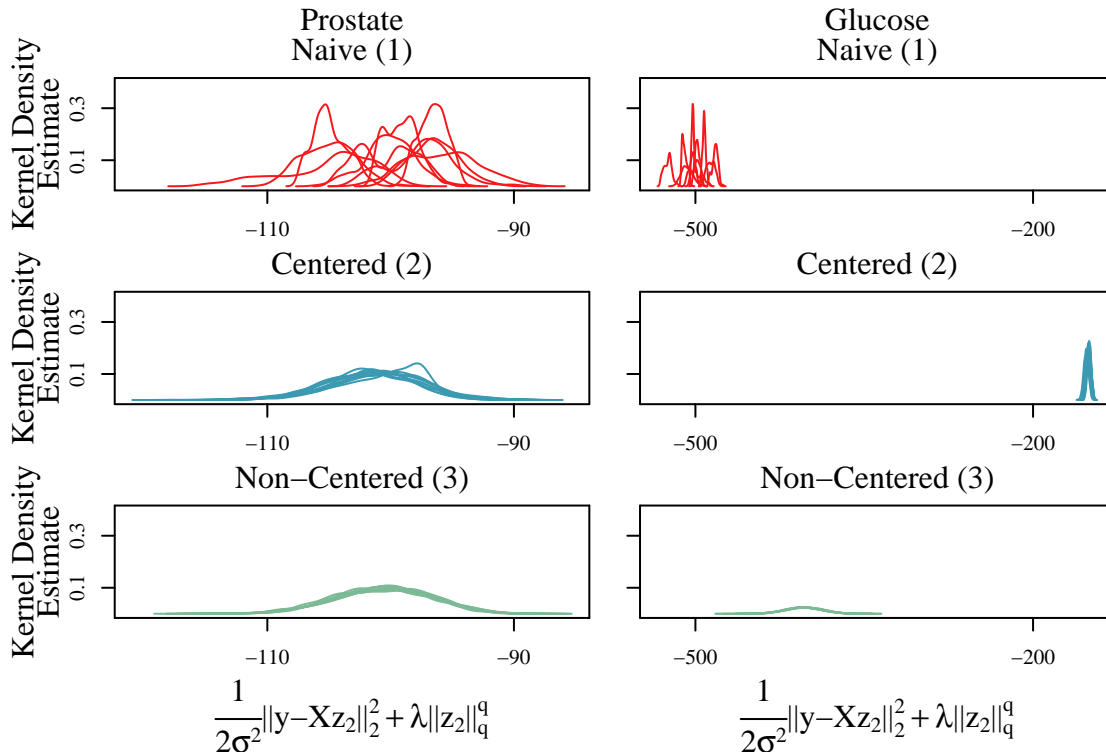


Figure 2: Kernel density estimates of the posterior density of the log unnormalized posterior $\mathbf{y} - \mathbf{X}\mathbf{z}_2\|_2^2/(2\sigma^2) + \lambda\|\mathbf{z}_2\|_q^q$ across chains for $q = 0.2$ based on 1,000 draws per chain after burn-in for the centered parametrization (2), the non-centered parametrization 3, and the naive parametrization (1) computed from the prostate and glucose datasets.

the non-centered parametrization (3). In contrast, the majority of chains obtained using centered parametrization (2) are consistent with the results obtained by using the non-centered parametrization (2), but one chain appears to get stuck at another incorrect mode. When the dimension of \mathbf{z}_2 is relatively large, the naive and centered parametrizations (1) and (2) do not share the same support as the non-centered parametrization (3). Both appear to get stuck far from the mode of the posterior distribution of $\|\mathbf{y} - \mathbf{X}\mathbf{z}_2\|_2^2/(2\sigma^2) + \lambda\|\mathbf{z}_2\|_q^q$.

Last, we examine divergent transitions after burn-in, which indicate numerical instability associated with draws from the posterior that can be interpreted as evidence of poor simulation performance (Carpenter et al., 2017). Divergences are prevalent for the centered parametrization (2), especially when q is small or the dimension of \mathbf{z}_2 is large. This is consistent with the performance of centered parametrizations in other settings (Betancourt and

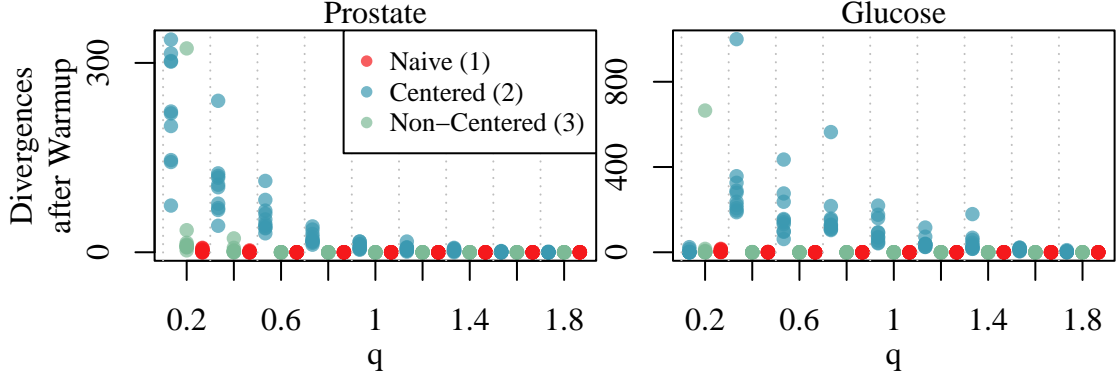


Figure 3: Divergent transitions after burn-in per chain for the centered parametrization (2), the non-centered parametrization 3, and the naive parametrization (1) computed from the prostate and glucose datasets.

Girolami, 2015). Interestingly, the naive parametrization (1) does not yield divergent transitions after warmup, even when it produces low effective sample sizes and poor estimates. This highlights the need to exercise care when using gradient-based methods to simulate from posterior distributions that are not differentiable.

3 Conclusion

In this note, we demonstrate the use of a latent variable representations of posterior distributions for random \mathbf{z} with densities proportional to $\exp\{f(\mathbf{z}) = g(\mathbf{z}) + \lambda\|\mathbf{z}_2\|_q^q\}$. This is of great value as it expands access to previously difficult to use models for users of STAN (Carpenter et al., 2017), PyMC (Salvatier et al., 2016), and other software for Hamiltonian Monte-Carlo based posterior simulation as described in Štrumbelj et al. (2024). This includes bridge penalized linear and generalized linear regression models, robust linear models of the form

$$\mathbf{y} = \mathbf{X}\beta + \mathbf{z}_2, \quad p(\mathbf{z}_2) \propto \exp\{-\lambda\|\mathbf{z}_2\|_q^q\},$$

and models that use the structured shrinkage priors introduced Griffin and Hoff (2024).

References

- Betancourt, M. and M. Girolami (2015). Hamiltonian monte carlo for hierarchical models. In S. K. Upadhyay, U. Singh, D. K. Dey, and A. Loganathan (Eds.), *Current Trends in Bayesian Methodology with Applications*, pp. 79–102. CRC Press.
- Butler, R. J., J. B. McDonald, R. D. Nelson, and S. B. White (1990). Robust and partially adaptive estimation of regression models. *The Review of Economics and Statistics* 72(2), 321–327.
- Carpenter, B., A. Gelman, M. D. Hoffman, D. Lee, B. Goodrich, M. Betancourt, M. A. Brubaker, J. Guo, P. Li, and A. Riddell (2017). Stan: A probabilistic programming language. *Journal of Statistical Software* 76(1), 1–32.
- Devroye, L. (2009). Random variate generation for exponentially and polynomially tilted stable distributions. *ACM Transactions on Modeling and Computer Simulation* 19, 1–20.
- Ding, P. and J. K. Blitzstein (2018). On the gaussian mixture representation of the laplace distribution. *The American Statistician* 72(2), 172–174.
- Frank, I. E. and J. H. Friedman (1993). A statistical view of some chemometrics regression tools. *Technometrics* 35, 109.
- Griffin, M. and P. D. Hoff (2020). Testing Sparsity Inducing Penalties. *Journal of Computational and Graphical Statistics* 29(1), 128–139.
- Griffin, M. and P. D. Hoff (2024). Structured Shrinkage Priors. *Journal of Computational and Graphical Statistics* 33(1), 1–14.
- Hans, C. (2009). Bayesian lasso regression. *Biometrika* 96, 835–845.
- Park, T. and G. Casella (2008). The bayesian lasso. *Journal of the American Statistical Association* 103, 681–686.

- Plummer, M. (2023). Simulation-based bayesian analysis. *Annual Review of Statistics and Its Application* 10(1), 401–425.
- Poirier, D. J., M. D. Tello, and S. E. Zin (1986). A diagnostic test for normality within the power exponential family. *Journal of Business & Economic Statistics* 4, 359–373.
- Polson, N. G., J. G. Scott, and J. Windle (2014). The bayesian bridge. *Journal of the Royal Statistical Society. Series B: Statistical Methodology* 76, 713–733.
- Priami, C. and M. J. Morine (2015). *Analysis of Biological Systems*. Imperial College Press.
- Salvatier, J., T. V. Wiecki, and C. Fonnesbeck (2016). Probabilistic programming in python using pymc3. *PeerJ Computer Science* 2, e55.
- Tibshirani, R. (1996). Regression shrinkage and selection via the lasso. *Journal of the Royal Statistical Society: Series B (Statistical Methodology)* 58, 267–288.
- Štrumbelj, E., A. Bouchard-Côté, J. Corander, A. Gelman, H. Rue, L. Murray, H. Pesonen, M. Plummer, and A. Vehtari (2024). Past, present and future of software for bayesian inference. *Statistical Science* 39(1), 46–61.
- West, M. (1987). On scale mixtures of normal distributions. *Biometrika* 74, 646–648.

Appendix

Let

$$\begin{aligned}
 k(\delta_i|q)^{\frac{q-2}{2q}} &= \left(\sin\left(\frac{q\delta_i}{2}\right)^{-\frac{q}{q-2}} \sin\left(\frac{(2-q)\delta_i}{2}\right) \sin(\delta_i)^{\frac{2}{q-2}} \right)^{\frac{q-2}{2q}} \\
 &= \sin\left(\left(\frac{q}{2}\right)\delta_i\right)^{-\frac{1}{2}} \sin\left(\left(\frac{2-q}{2}\right)\delta_i\right)^{\frac{q-2}{2q}} \sin(\delta_i)^{\frac{1}{q}}.
 \end{aligned}$$

If $p(\mathbf{z}_2) = \frac{q}{2\Gamma(1/q)\lambda^{-1/q}} \exp\left\{-\lambda \|\mathbf{z}_2\|_q^q\right\}$, then

$$\begin{aligned}
p(\mathbf{z}_2|\boldsymbol{\xi}) p(\boldsymbol{\xi}|\boldsymbol{\delta}) p(\boldsymbol{\delta}) &= \prod_{j=1}^{n_2} \left(\frac{\pi \left(\frac{\xi_j}{k(\delta_j|q)} \right)^{\frac{2-q}{q}}}{\lambda^{\frac{2}{q}}} \right)^{-\frac{1}{2}} \exp \left\{ -\frac{z_{2j}^2 \lambda^{\frac{2}{q}}}{\left(\frac{\xi_j}{k(\delta_j|q)} \right)^{\frac{2-q}{q}}} \right\} \left(\frac{1}{\Gamma\left(\frac{2+q}{2q}\right)} \right) \\
&\quad (\xi_j)^{\frac{2+q}{2q}-1} \exp\{-\xi_j\} \\
&\quad \left(\frac{\Gamma\left(1 + \frac{1}{2}\right) \Gamma\left(\frac{1}{2} + \frac{1}{q}\right)}{\pi \Gamma\left(1 + \frac{1}{q}\right)} \right) k(\delta_j|q)^{\frac{q-2}{2q}} \\
&= \prod_{j=1}^{n_2} \left(\frac{1}{2\pi} \right) \left(\frac{q\lambda^{\frac{1}{q}}}{\Gamma\left(\frac{1}{q}\right)} \right) \times \\
&\quad \exp \left\{ -\xi_j - \lambda^{\frac{2}{q}} z_{2j}^2 \xi_j^{\frac{q-2}{q}} \sin\left(\left(\frac{q}{2}\right)\delta_j\right)^{-1} \sin\left(\left(\frac{2-q}{2}\right)\delta_j\right)^{\frac{q-2}{q}} \sin\left(\delta_j\right)^{\frac{2}{q}} \right\},
\end{aligned}$$

where $\Gamma(1 + 1/q) = \Gamma(1/q)/q$ and $\Gamma(3/2) = \pi^{1/2}/2$ follow from properties of the gamma function as described in Abramowitz and Stegun.

An alternative, set $\mathbf{z}_2 = \left(\frac{\boldsymbol{\xi}^{\frac{2-q}{2q}}}{\sqrt{2}\lambda^{\frac{1}{q}} k(\boldsymbol{\delta}|q)^{\frac{2-q}{2q}}} \right) \mathbf{w}$ and simulate from:

$$\begin{aligned}
p(\mathbf{w}_2|\boldsymbol{\xi}) p(\boldsymbol{\xi}|\boldsymbol{\delta}) p(\boldsymbol{\delta}) &= \prod_{j=1}^{n_2} (2\pi)^{-\frac{1}{2}} \exp \left\{ -\frac{w_j^2}{2} \right\} \left(\frac{1}{\Gamma\left(\frac{2+q}{2q}\right)} \right) \\
&\quad \xi_j^{\frac{2+q}{2q}-1} \exp\{-\xi_j\} \\
&\quad \left(\frac{\Gamma\left(1 + \frac{1}{2}\right) \Gamma\left(\frac{1}{2} + \frac{1}{q}\right)}{\pi \Gamma\left(1 + \frac{1}{q}\right)} \right) k(\delta_j|q)^{\frac{q-2}{2q}} \\
&= \prod_{j=1}^{n_2} \left(\frac{1}{2^{\frac{3}{2}}\pi} \right) \left(\frac{q}{\Gamma\left(\frac{1}{q}\right)} \right) \exp \left\{ -\frac{w_j^2}{2} \right\} \\
&\quad \xi_j^{\frac{2-q}{2q}} \exp\{-\xi_j\} \sin\left(\left(\frac{q}{2}\right)\delta_j\right)^{-\frac{1}{2}} \sin\left(\left(\frac{2-q}{2}\right)\delta_j\right)^{\frac{q-2}{2q}} \sin\left(\delta_j\right)^{\frac{1}{q}}
\end{aligned}$$

where $\Gamma(1 + 1/q) = \Gamma(1/q)/q$ and $\Gamma(3/2) = \pi^{1/2}/2$ follow from properties of the gamma function as described in Abramowitz and Stegun.